

Synchrotron X-Ray Study of the Commensurate-Incommensurate Transition of Monolayer Krypton on Graphite

D. E. Moncton

Bell Laboratories, Murray Hill, New Jersey 07974

and

P. W. Stephens^(a) and R. J. Birgeneau

Department of Physics, Massachusetts Institute of Technology, Cambridge, Massachusetts 02139

and

P. M. Horn

IBM Research Center, Yorktown Heights, New York 10598

and

G. S. Brown

Stanford Synchrotron Radiation Laboratory, Stanford, California 94305

(Received 29 January 1981)

We report a high-resolution synchrotron x-ray scattering study of the commensurate-to-incommensurate transition of monolayer krypton physisorbed on *ZYX* graphite. At the transition the substrate-limited coherence of the commensurate monolayer (2300 Å) deteriorates to less than 100 Å, demonstrating that atomic positional disorder is a dominant feature of the weakly incommensurate system. The peak position follows a $\frac{1}{3}$ power law versus reduced temperature.

PACS numbers: 68.55.+b, 61.10.-i, 64.70.Dv

The utilization of intense, highly collimated beams of synchrotron x radiation for high-resolution scattering studies is now technically possible. Since this technique is capable of spanning the spatial resolution scale from 1 Å to >10 000 Å, it has great potential for the study of the development of correlations near structural phase transitions. We have chosen to investigate the commensurate-incommensurate transition (C-IT) of monolayer krypton on graphite which has been the subject of a number of previous experimental studies.^{1,2} In turn these experiments have inspired a variety of theoretical calculations.³ In previous low resolution (~ 0.01 Å⁻¹) x-ray studies, Stephens *et al.*² characterized the C-IT behavior as a second-order transition from the hexagonal commensurate structure to a hexagonal incommensurate solid phase. Near the transition, the scattering from the incommensurate phase was interpreted as a Bragg reflection from the average incommensurate lattice and an accompanying satellite reflection due to modulation by the graphite substrate. The incommensurability ϵ was shown to follow a simple universal power law,^{1,2}

$$\epsilon \sim \epsilon_0 (1 - \mu/\mu_c)^{0.29 \pm 0.04},$$

over a wide range of temperatures. A puzzling feature in the previous diffraction studies was that the incommensurate profiles were somewhat

broader than the commensurate profiles.

In this paper we report a much-higher-resolution (~ 0.0004 Å⁻¹) study using synchrotron x-ray radiation. We show that the broadening is the most important feature of the C-IT. Unexpectedly, the weakly incommensurate phase is disordered at temperatures well below the anticipated solidification temperature at these densities. The correlation lengths deduced from peak widths imply that the incommensurate phase is unusually well correlated for a liquid, but it is clearly not a two-dimensional (2D) solid. In spite of this new picture of the transition, the present measurements yield a power-law dependence for the incommensurability, $\epsilon = \epsilon_0 (1 - T/T_c)^{1/3}$, equivalent to that previously observed.² These results clearly require new theories for the C-IT.

We performed experiments at the Stanford Synchrotron Radiation Laboratory using the Bell Laboratories x-ray diffraction spectrometer stationed on beamline II. The radiation was focused onto the sample with use of an ellipsoidal x-ray mirror. We used two parallel germanium (111) crystals to monochromatize the incident beam ($\lambda \sim 1.7$ Å) and a single germanium (111) crystal to analyze the diffracted beam. The longitudinal resolution was 3.5×10^{-4} Å⁻¹ half-width at half maximum (HWHM) and the out-of-plane resolution was 0.015 Å⁻¹ HWHM. The longitudinal reso-

lution corresponds to a particle size of about 9000 Å. For the substrate we employed Union Carbide ZYX exfoliated graphite, as discussed previously.² We used a single $1.2 \times 1.2 \times 0.2$ cm³ plate with the *c* axis, which is normal to the plate, in the scattering plane. Only the center (0.02 cm³) was exposed to x rays.

The krypton-gas-handling system and cryostat were similar to those discussed by Horn *et al.*² Here, however, we used a large sample cell in which about 50% of the krypton was in the 3D vapor phase at melting. Temperature scans were carried out in a closed cell and hence both the chemical potential and the surface density varied. Except for the data of Fig. 1, the krypton content in the cell was such that the liquid-to-commensurate solid and commensurate-to-incommensurate transitions occurred at temperatures of 112.9 and 97.24 K, respectively. The commensurate melting transition and the line shape in the commensurate ($\sqrt{3} \times \sqrt{3}$)R30° phase have been discussed elsewhere.⁴

As shown at the top of Fig. 2, the commensurate line shape is well described by a Gaussian with a 0.0014 Å⁻¹ HWHM which corresponds to a particle size $L = \pi/(\text{HWHM}) = 2300$ Å. The behavior as a function of decreasing temperature (increasing coverage) is shown in Fig. 2. Near 97.5 K the line profile develops a composite shape

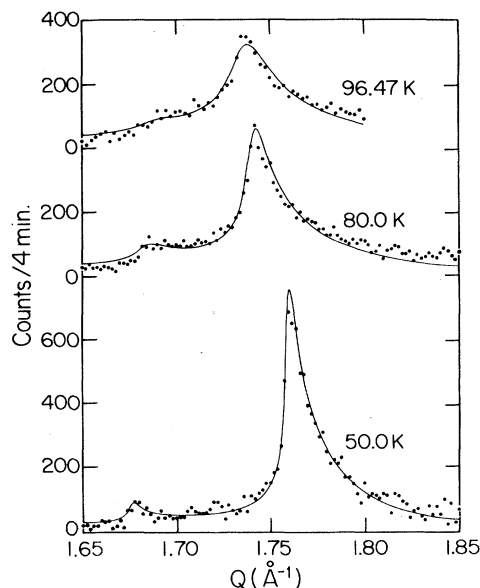


FIG. 1. Krypton (10) diffraction profiles at three temperatures; the amount of gas in the cell was different for each scan. The solid lines are all results of fits to a model with Lorentzians at $Q = Q_{\text{comm}} + \epsilon$ and $Q = Q_{\text{comm}} - \epsilon/2$.

with a sharp component whose intensity decreases rapidly with decreasing temperature and a broad component which is only weakly temperature dependent. This structure is not fully understood and requires further study. As the temperature is lowered to 97.24 K the sharp component disappears entirely and one is left with a broad, slightly incommensurate peak indicative of a liquidlike state. With decreasing temperature the peak moves to larger *Q*, initially broadening, but then narrowing as the incommensurability increases further. At large incommensurability, the width begins to approach that of the commensurate line shape. Furthermore, measurements of xenon, with a factor-of-2 larger incommensurability ($\epsilon \sim 0.1$ Å⁻¹), show a profile as sharp as commensurate krypton. Therefore, at large incommensurability, we are apparently near a transition to an incommensurate 2D solid. Clearly this behavior is much more elaborate than had previously been supposed.^{1,2,3}

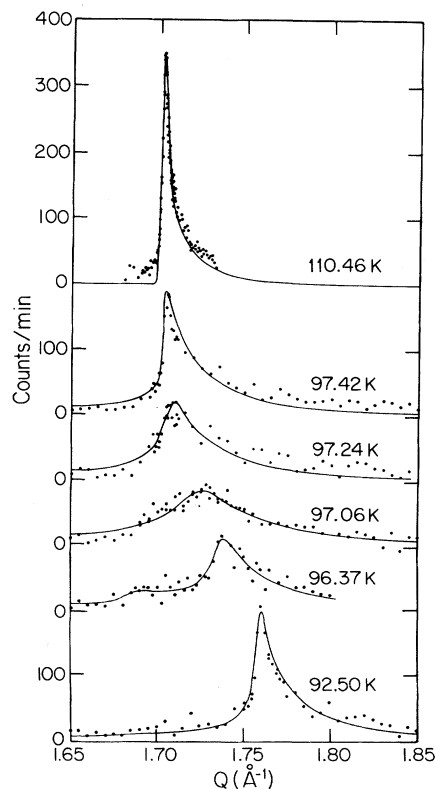


FIG. 2. Krypton (10) diffraction profiles at a number of temperatures; the empty-cell background has been subtracted. The solid lines are theoretical fits as discussed in the text.

In Fig. 1, we show scans with varied incommensurability at several temperatures down to 50 K. These data show that the peak at $+\epsilon$ is accompanied by an additional feature at $-\epsilon/2$ which becomes better defined as the correlation increases at lower temperatures. The peak at $-\epsilon/2$ undoubtedly results from the modulation of the Kr lattice by the graphite substrate. If this modulation consisted of a perfectly ordered array of domain walls that were considerably narrower than the average distance between them, the intensity ratio would be $I(-\epsilon/2)/I(+\epsilon) = 2$, considerably greater than that observed. On the other hand, a simple model of sinusoidal modulation may not be able to account for intensity ratios as large as those observed. We conclude that an intermediate description of the Kr system is probably best at these temperatures.

The most remarkable feature of our data is the positional disorder of the weakly incommensurate phase. This result is extremely surprising since the heat capacity data of Butler, Litzinger, and Stewart⁵ imply that the melting temperature at this coverage should be above 120 K. We observe this liquidlike behavior down to at least 80 K. It is evident therefore that the line broadening observed previously as a subtle aspect of the data is, in fact, the most important feature. To analyze these data quantitatively we have assumed a Lorentzian line profile for the structure factor

$$S(\vec{Q}) = \frac{A}{\kappa^2 + (\vec{Q} - \vec{Q}_0)^2}. \quad (1)$$

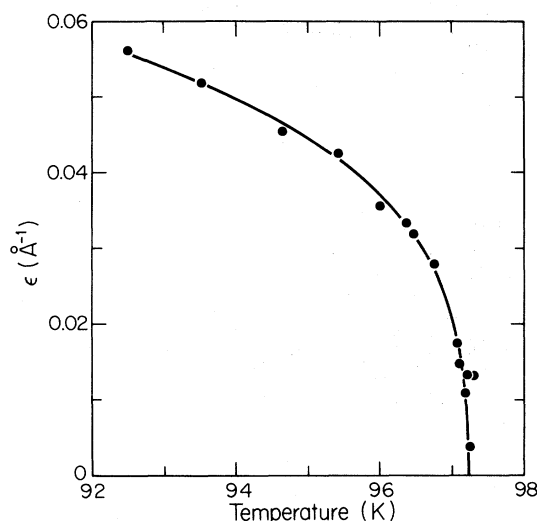


FIG. 3. Incommensurability ϵ vs temperature. The solid line is the power law $\epsilon = \epsilon_0(1 - T/T_c)^\beta$, with $\beta = 0.33 \pm 0.03$, $T_c = 97.23 \pm 0.03$, and $\epsilon_0 = 0.155 \text{ \AA}^{-1}$.

The azimuthal powder average of Eq. (1) can be calculated exactly. This cross section is then convoluted with the vertical mosaic distribution of crystallites and the instrumental resolution function. Near T_c , a single Lorentzian peak at $\vec{Q}_0 = \vec{Q}_{\text{comm}} + \epsilon$ is adequate. However, for incommensurability greater than 0.02 \AA^{-1} it is necessary to include a second weaker peak with width κ at $\vec{Q}_0 - 3\epsilon/2 = \vec{Q}_{\text{comm}} - \epsilon/2$, where \vec{Q}_{comm} is the (10) lattice vector for the $(\sqrt{3} \times \sqrt{3})R30^\circ$ structure. The solid lines in Figs. 1 and 2 for the data below 97.42 K are the results of such fits. In these fits \vec{Q}_0 , κ , and two amplitudes are adjusted while the background is fixed by empty-cell scans. Within the statistics of our data, this model works quite well. Only at the highest incommensurabilities do the peaks attain a width as small as that in the commensurate phase. Even then, as shown in the scans at 110.46 K in Fig. 2 and at 50 K in Fig. 1, there is a marked difference between the Lorentzian line shape which best fits the incommensurate data, and the Gaussian line shape of the commensurate phase. This tendency is consistent with the tails expected from the power-law correlations in an incommensurate 2D solid.

The parameters obtained from our fits are shown in Figs. 3 and 4. The solid line in Fig. 3 shows a least-squares fit of a power-law form $\epsilon = \epsilon_0(1 - T/T_c)^\beta$ to our synchrotron data. The best-fit exponent is $\beta = 0.33 \pm 0.03$, which agrees within the errors with the previous results.^{1,2} Thus this simple power-law behavior is observed for scans both in temperature and in chemical potential although the incommensurate phase is

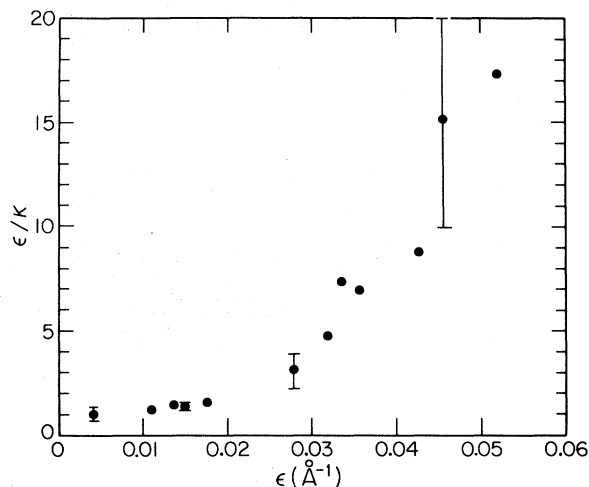


FIG. 4. Incommensurability ϵ divided by the fitted Lorentzian HWHM κ vs ϵ .

initially disordered.

We show in Fig. 4 the ratio of the incommensurability, ϵ , to the HWHM of the Lorentzian, κ , plotted versus ϵ . For small incommensurabilities, ϵ/κ is a constant near unity. Then, as ϵ increases above 0.02 \AA^{-1} , this ratio increases rapidly. In the absence of theoretical calculation of structure factors for any model of the disordered incommensurate phase, it is difficult to interpret this behavior quantitatively. However, a few general remarks are necessary. Before our experiments, only one theoretical model proposed a disordered incommensurate phase.³ It consisted of a "breathing" honeycomb network of domain walls. Motivated by our experiments, Coppersmith *et al.*⁶ have shown that such an incommensurate phase would have a power-law structure factor, $S(\vec{Q}) \sim (\vec{Q} - \vec{Q}_0)^{-2+\eta}$, rather than the observed broad Lorentzian. More importantly such a phase would be unstable to the formation of free dislocations and hence is a liquid. For a sufficiently weak incommensurability a fluid phase may be possible at all temperatures. These calculations are based on a domain-wall picture, however, which may not be appropriate for this system. In spite of this uncertainty, the experimental fact that the ratio ϵ/κ approaches unity near the C-IT is an essential feature of the weakly incommensurate liquid. Furthermore, it is known that the amount of extra Kr adsorbed scales (within 20%) with the incommensurability ϵ . Therefore we conclude that the coherence of the weakly incommensurate state is such that κ^2 is roughly equal to the extra Kr density.

In summary, the weakly incommensurate phase exhibits a liquidlike structure factor at temperatures far below the expected melting temperature. We believe that it is only the weak incommensurability of the system that is fundamental to its disordered nature, not the explicit form of the substrate-induced modulation. Clearly a finite-temperature theory is required which addresses the

structure of the incommensurate phase as one moves away from the domain-wall model toward the sinusoidal modulation limit. Finally, we note that use of a synchrotron source has enabled us to improve our resolution by a factor of 20 and elucidate physics which was entirely unexpected.

We wish to acknowledge helpful discussions with W. F. Brinkman, D. S. Fisher, and P. A. Lee. We should also like to thank the Stanford Synchrotron Radiation Laboratory staff for their generous assistance. This work done at Massachusetts Institute of Technology and Stanford Synchrotron Radiation Laboratory was supported in part by the Joint Services Electronics Program under Contract No. DAAG-29-80-C-0104 and by the National Science Foundation under Contract No. 77-27489.

^(a)Present address: Department of Physics, S.U.N.Y. at Stony Brook, Stony Brook, N. Y. 11794.

¹M. D. Chinn and S. C. Fain, Jr., *Phys. Rev. Lett.* **39**, 146 (1977); S. C. Fain, Jr., M. D. Chinn, and R. D. Diehl, *Phys. Rev. B* **21**, 4170 (1980).

²P. W. Stephens, P. Heiney, R. J. Birgeneau, and P. M. Horn, *Phys. Rev. Lett.* **43**, 47 (1979); R. J. Birgeneau, E. M. Hammonds, P. Heiney, P. W. Stephens, and P. M. Horn, in *Ordering in Two Dimensions*, edited by S. K. Sinha (Plenum, New York, 1980), and references therein.

³For a review, see J. Villain, in *Order in Strongly Fluctuating Condensed Matter Systems*, edited by T. Riste (Plenum, New York, 1980), p. 221.

⁴R. J. Birgeneau, G. S. Brown, P. M. Horn, D. E. Moncton, and P. W. Stephens, to be published.

⁵D. M. Butler, J. A. Litzinger, and G. A. Stewart, *Phys. Rev. Lett.* **44**, 466 (1980).

⁶S. N. Coppersmith, D. S. Fisher, B. I. Halperin, P. A. Lee, and W. F. Brinkman, *Phys. Rev. Lett.* **46**, 549 (1981); P. Bak, *Phys. Rev. Lett.* **46**, 791 (1981) relate specifically to this problem. Other relevant theoretical treatments are contained in S. Ostlund, *Phys. Rev. B* **23**, 2235 (1981); S. T. Chui, T. Ohta, S. Ostlund, and J. Villain, to be published.